Solar Energy Advances 2 (2022) 100022

Contents lists available at ScienceDirect

Solar Energy Advances

journal homepage: www.elsevier.com/locate/seja

Urban cooling technologies potential in high and low buildings densities

Cláudia Cotrim Pezzuto [a], Noelia Liliana Alchapar [b,*], Erica Norma Correa [b]

[a] Urban Infrastructure Graduation Program, Pontifical Catholic University of Campinas, Rodovia D. Pedro I, km 136, Parque das Universidades, Campinas, SP, 13086-900, Brazil

[b] Institute of Environment, Habitat and Energy (INAHE-CONICET). CCT Mendoza, CC, 131 5500 Mendoza, Argentina

ARTICLE INFO

Keywords:
High albedo
Urban vegetation
Building density
Anthropogenic heat
Urban heat island
Mitigations strategies

ABSTRACT

To mitigate the temperature increase in urban environments and reduce its impact on energy consumption and the quality of the environment, urban retrofitting technologies have been developed and applied worldwide. High albedo in urban surfaces and additional vegetation are the most efficient strategies to accomplish these goals. The objective of this study is to estimate the weight of these strategies, both individually and integrated, on the cooling potential of two Latin American cities. To do this, 36 low and high urban density scenarios were simulated with the ENVI-Met software. The simulation models were calibrated using air temperature curves which were monitored during the summer periods from 2010 to 2013. A Principal Components Analysis was carried out to establish possible associations between the proposed mitigation strategies and then the weight of anthropogenic heat was evaluated according to the configuration. The results show that the integrated mitigation strategies in urban areas -i. e. increase vegetation and albedo on horizontal surfaces- has a great potential to mitigate urban warming, showing a more significant impact on low-density urban configuration. The contribution of anthropogenic heat mainly produced by motorized transport and air conditioning systems, is a crucial input data for the urban microclimate simulations. Its impact on the urban densification processes may cancel out the benefits derived by the application of the mitigation strategies considered.

1. Introduction

Increasing urban warming is an indicator of the unsustainable path urban development has taken around the world. Urban growth and expansion have generated a set of adverse effects and environmental risks, widely analyzed during the last decades [1]. In this scenarios, the world's climate system is getting warmer [2]. According to the Intergovernmental Panel on Climate Change [3], global mean surface air temperature is projected to increase from 0.3˚ to 4.8˚C by the year 2100, depending on the specific emission scenario and the climate model. Since climate change is expected to generate more intense and frequent heat waves, it is essential to develop and implement comprehensive heat mitigation strategies for urban areas.

In urban areas, urbanization leads to the urban heat island (UHI) effect, which is defined as an increase in the urban air temperature when compared to their rural surroundings [4]. UHI is caused by numerous reasons, including the thermal and optical properties of the materials used in cities, the morphology of urban canyons, the concentration of released anthropogenic heat, the urban greenhouse effect, the reduction of evaporative surfaces, and the turbulence phenomena caused by the increase in building density [5]. This climatic vulnerability within cities increases the cooling loads of buildings and reduces thermal comfort both inside buildings [6] and in outdoor space, potentially causing serious health conditions for its inhabitants [7].

Adaptation and mitigation technologies have been developed and applied to counteract the temperature increase in urban environments and to reduce their impact on energy consumption and environmental quality. Among the most efficient urban retrofitting technologies are the use of high albedo surfaces and increase urban vegetation [8]. Studies carried out in the same areas of this research, can reduce the maximum air temperature by approximately 2˚C to 3˚C in the cities of Mendoza (Argentina) and Campinas (Brazil) [9]. A further reduction can be achieved in neighborhoods by employing advanced evaporation [10]. In addition, they have a positive impact on the thermal comfort of urban spaces, on the reduction of consumption and rational use of energy, and on the reduction of CO_2 emissions [11–13].

The increase in urban albedo, under certain conditions, contributes to reducing not only urban overheating and UHI effect in cities, but also the local air temperature peak [14,15]. Cool or highly-reflective materials are defined as materials with high solar reflectance and high emissivity in the infrared region of the solar spectrum [16]. Numerous studies investigate the benefits of using cool roofs, façades and pavements.

* Corresponding author at: CONICET: Consejo Nacional de Investigaciones Cientificas y Tecnicas, Argentina.
E-mail address: nalchapar@mendoza-conicet.gob.ar (N.L. Alchapar).

https://doi.org/10.1016/j.seja.2022.100022
Received 15 September 2021; Received in revised form 17 August 2022; Accepted 23 August 2022
Available online 27 August 2022

The use of these reflective technologies can reduce the maximum air temperature by 2.3°C in cool roofs, 2.5°C in cool pavements and 3.4°C in both surfaces [10,11,17,18]. Besides this, it causes maximum reductions in surface temperatures of around 39°C on façades [19], from 21° to 41°C on roofs [19,20], and 32°C in pavements [21]. In relation to thermal comfort, studies have shown that cool materials can improve or worsen the conditions of the space depending on the climate and the composition - morphological and material - of the analyzed space [22]. The efficiency of these materials is conditioned by the relative position within a road channel. Horizontal surfaces (roofs and floors) are better radiators of heat energy into the atmosphere. However, the application of cool materials on the facades can excessively raise the average radiant temperature (Tmr), causing serious problems regarding thermal discomfort [15]. In the city of Mendoza, Argentina, with a temperate arid climate, raising the albedo of facades from 0.3 to 0.8 in a forested road channel causes a growth of the Tmr of up to 17°C in low density (H/W aspect:0.3) and up to 23°C in high density (H/W aspect:1.5). In contrast, in a vial canyon without afforestation, Tmr increases reach 27°C [23]. This effect is called the Inter-Building Effect (IBE) and it is enhanced in deep urban profiles without afforestation [24].

In Campinas city, Abreu-Harbich [25] reports the effect of climate mitigation and reduction in energy consumption caused by afforestation in urban canyons. Research carried out by Ruiz and Correa [26] showed that an adequate combination between the width of the urban canyon and the forest species, which favors the distribution of shadows and wind circulation, minimizes the consumption of auxiliary building energy by up to 30% in summer.

Numerous studies have been carried out to identify the cooling potential of both reflective technologies and green infrastructure to mitigate urban overheating and improve urban comfort [22,27–29]. However, knowledge of the potential of the simultaneous combination of both strategies is limited and their efficiency is highly dependent on the climate and the structure of the city where they are applied [29,30].

Additionally, it is well known that the anthropogenic heat (AH) generated by human activities has a great impact on the urban and climate. The UHI can be influenced not only by physical and geometric factors such as roughness, thermal inertia and sky view factor, but also by meteorological conditions such as wind speed, cloudiness, relative humidity and the stability of the atmospheric boundary layer. While the amount of energy released as a result of anthropogenic activities is a tiny fraction of the sun energy intercepted by the earth on a global scale, it is recognized that the density of human energy production can be substantially higher in urban regions. AH sources include heat generated by the combustion process in vehicles, heat emitted by industrial processes, heat conduction through building walls, heat emitted directly into the atmosphere by air conditioning systems, and metabolic heat produced by humans. The amount of heat supplied is influenced by climate and time, as these determine whether heating or cooling systems are used [31]. Various investigations have identified numerous consequences of UHI, including negative impacts on public health, decreased community well-being, reduced economic activity, increased energy use, and increased heat stress in public spaces [32–34].

The AH generated by human activities in urban areas can have a significant influence on the dynamics and thermodynamics of the city boundary layer [35,36]. The mean annual temperature and the height of the planetary boundary layer are expected to increase, particularly in regions where the AH flux exceeds the threshold of 3 W m^{-2} [37]. Besides, the increase in air temperature due to the introduced heat can intensify local circulations and photochemical processes that generate pollution [38]. There is a growing body of research concerned with the impact of anthropogenic thermal pollution upon the dynamics of the urban boundary layer [39–41].

According to Sailor and Lu [42], most cities have maximum anthropogenic residual heat values between 30 and 60 W/m2 (city-wide averages). The diurnal cycle of the urban AH flux averaged globally ranges from 0.7 to 3.6 W m^{-2} [43]. Several cities have been evaluated, for instance, the mean annual value for Greater London has been estimated at 10.9 W m^{-2} [44] while for Seoul it has been estimated at 55 W m^{-2} [45]. Smith et al. [46], estimates a mean heat emission of 6.12 Wm^{-2} across Greater Manchester, with values in the region of 10 Wm^{-2} for non-central urbanized areas and 23 Wm^{-2} in city center areas. This study also states that buildings represent the dominant emitter, contributing some 60% of the emissions across the city, compared to around 32% for road traffic and 8% for metabolic sources.

Despite its local importance, AH is frequently omitted from climate models [43]. In relation to the incorporation of AH flux in microclimatic simulation models, progress has been made during the last decade because it is imperative to include this variable in order to build more robust models which are calibrated to the processes of the urban canopy -layer close to the urban surface-. At that level, flows become completely three-dimensional, transient, intermittent and much more complex than the two-dimensional turbulences. Furthermore, they are considered in most of the equations used by current urban simulation models [47]. Among the latest advances to integrate human dimension models in meteorological and climate models, Masson et al. [48] incorporated building energy demand data in urban simulations. Moreover, Xu et al. [49] proposed a parameter called Cooled Fraction in the WRF - Urban software to estimate the electrical loads of air conditioning-, considering the heterogeneity in building occupancy parameters (hours and densities of use). In addition, Capel-Timms et al. [50] developed a model to dynamically calculate building energy heat fluxes from neighborhood scale parameters.

In this frame, we can affirm that the understanding of the AH flux is well summarized and developed in the international literature; and that its incorporation in urban climate simulation models is relatively straightforward, involving the addition of a source/sink term, usually constant, in the surface and the control volume of energy budget equations [51]. However, the impact of this flux is often not considered in studies that evaluate the result of the implementation of diverse mitigation strategies to improve the thermal environment [11]. According to the information previously discussed, it would be important to include the AH flux effect when evaluating the impact derived from the implementation of several mitigation strategies over urban air temperatures. In particular, those strategies that involve an urban density increase, due to a major building density, are frequently followed by an increase of AH flux.

Finally, the presence of the UHI phenomenon and its characterization in Latin American cities have been widely documented [52,53]. In the city of Mendoza, the maximum intensity of UHI ranges between 8° and 10°C, with an average value of 6°C [54]. In the city of Campinas, a heat island´s intensity in winter is approximately 5°C while in summer it is 3.5°C [55,56]. It has also been proven that the shape of the air temperature curve is similar to the shape of the solar radiation curve of the exposed facade. Thus, from the point of view of the bioclimatic conditioning of spaces, it is advisable to work on the shading of the façades and on their surface properties [54]. Considering that 90% of the Latin American population resides in urban areas [57] it is of particular interest to discuss the efficiency of the application of different urban retrofitting strategies to mitigate urban overheating.

This research gives continuity to the research started in Alchapar et al. [9] that sought to quantitatively determine which cool strategies are the most effective in the cities of Campinas (Brazil) e Mendoza (Argentina). The objective of this study is to verify whether the effect of urban cooling is enhanced by integrating urban surfaces with high albedo and a higher percentage of green infrastructure, taking into account the AH flux impact associated to the implementation of each strategy analyzed. To do this, we compare the thermal variations of 36 urban scenarios in high and low density during the summer period. The study was carried out in two Latin American cities, Campinas – Brazil, with Cwa-Köppen climate classification and Mendoza – Argentina, with BWh-Köppen climate classification [58].

Table 1
General information features of Campinas (C) and Mendoza (M) city.

General features	Campinas (C)	Mendoza (M)
Geographical coordinates	S 22°53′20", W 47°04′40"	S 32°54′48", W 68°50′46
Average altitude (meters)	680	750
Population (inhabitants)	1,223,237	1,115,041
Local Climate Zones (LZC)	36: Compact low-rise with Open low-rise	6: Open low-rise with dense trees
Mean annual rainfall (mm)	116	244
Köppen climatic classification	Cwa: hot and humid summers and dry winters	BWh: warm desert
Average annual air temperature (°C)	22.4	17.8
Average annual minimum temperature (°C)	12.4	5.7
Average annual maximum temperature (°C)	32.5	31.5
Average annual wind velocity at 2 m (meters/seconds)	2.2	1.9

Reference: [56,59–61].

2. Methods

In this research, methods for monitoring microclimatic conditions and computer simulation methods were used to evaluate the potential of the combination of albedo and vegetation as a strategy to mitigate urban warming during the summer period. For the case study, two areas were selected: one in the city of Campinas, Brazil, and the other in the city of Mendoza, Argentina. Both are characterized by having a residential and commercial use, low building density and proximity to the urban center.

The methodology has been structured in four sections:

1 Characteristics of the study area and climate monitoring: Description of the climate monitoring process carried out in the study areas.
2 Model input parameters: Description of simulation process with ENVI-met software.
3 Simulation model calibration: The model is set according to the observed air temperature curve in receptor R1.
4 Characterization of the study scenarios: Description of the 36 scenarios proposed for the simulation.

2.1. Characteristics of the study area and climate monitoring

Two Latin American cities with warm climate and similar morphological parameters were selected as study areas. Campinas is located in the southeast of Brazil. Mendoza is located in the center-west of Argentina. The general characteristics are detailed in Table 1.

The two study areas are regions of low density and proximity to the urban center with representative morphological patterns of areas of residential, commercial use. Air temperature was monitored through a sensor installed in the urban canyons located in the center of each area (Fig. 1). The field measurements were carried out in the summer period, on clear days with low wind speed (≥3 meters /seconds at 10 meters high) and without rainfall occurrence. In the city of Campinas, data collection was carried out on February 21, 2013. The data from the meteorological station (Campinas Agronomic Institute -IAC) were: maximum air temperature 31.4°C, minimum air temperature 18.2°C, mean air temperature 23.2°C, relative humidity 66.8% and mean maximum global radiation of 925.0 W/m^2. In Mendoza, the collection took place on January 14, 2010. The data from meteorological station (Observatory of Francisco Gabrielli Airport) were: maximum air temperature 31.0°C, minimum air temperature 22.0°C, average air temperature 26.0°C, relative humidity 39%, and average maximum global solar radiation of 1,181.0 W/m^2.

The monitoring point (receptor R1) was set inside the urban canyon at an approximate height of 2.5 meters, avoiding the proximity of obstacles. The instrumentation used in the city of Campinas was a Testo 174 H sensor (temperature range -20°C to 70°C, resolution of 0.1°C and precision of 0.5°C), while a HOBO H08- 003-02 sensor (temperature range -20°C to 70°C, 0.1°C resolution and 0.7°C accuracy) was used in Mendoza. The sensors were inside protectors that prevent direct incidence of solar radiation (HOBO RS1 Solar Radiation Shield). Table 2 details the morpho-material features of each city.

2.2. Model inputs parameters

The microclimate of each study area was simulated with the ENVI-Met software developed by Michael Bruse [62] which is an auspicious and widely used tool in microclimate studies [9,18,63,64]. This software uses air flow models, turbulence, profiles of temperature and humidity and radiation flows which occur between the atmosphere and surfaces near the ground [65,66]. The model is a useful and internationally validated prediction tool for evaluating air temperature response to different configurations of urban space. However, it is necessary to adequately detail the study area and know its limitations for the interpretation and analysis of the results [67].

The study areas considered an extent of 210 × 210 meters, in which cells with a resolution of 3 meters were adopted to maintain a good model precision obtaining a 70 × 70 analysis grid. The total height of the model was 30 meters for both cities in accordance to the ENVI-Met Guide [68] which states that the minimum height required is twice the height of the tallest building and a minimum of 30 meters. To maintain stability, 5 nesting grids were inserted around the model [66].

Table 3 shows the input parameters in the ENVI-Met software for the configuration file: wind speed and direction -at 10 meters- and relative humidity -at 2 meters high-. The reference urban weather stations are located 2.2 km northwest of Campinas´ study area (Campinas Agronomic Institute -IAC), and 3.2 km northwest of Mendoza´s study area (Mendoza Observatory Meteorological). The average values recorded in the evaluated urban canyons were adopted for the thermal properties of the buildings. The specific humidity data at 2.5 meters high was collected in 83779 and 87418 meteorological station numbers, Campinas and Mendoza respectively.

For the assessment, 126 hours were simulated and the theoretical model was stabilized at 96 hours. That is why the results considered within this analysis correspond to run number 4 of the model. The simulation was set to start at 9 p.m., to avoid influence on solar radiation in the first simulated data. Indoor building temperatures were set at 24.85°C in Campinas and 25.85°C in Mendoza. These values were adopted because they correspond to the operating temperature that a building could reach in summer, without consuming auxiliary energy for refrigeration. These values are not far from the recommended summer comfort temperature for each city [30]. According to the limitations of the outdoor climatic conditions, this average operating temperature could be reached by means of passive cooling techniques without the need to consume aux energy. If there was consumption, it should be considered for the calculation of the anthropic contribution.

For the characterization of the vegetation, the ENVI-Met default database was used, according to the vegetation features in both cities. To adjust the percentage of vegetation in the theoretical model, digital hemispheric images of the urban canyons of both cities were collected and the sky view factor (SVF) was calculated. Next, the simulated SVF was adjusted with the SVF measured in the real condition. In addition to the SVF, the vegetation selection also included the analysis of the leaf area index (LAD) of the vegetation in the areas and the choice of the most appropriate one based on those proposed in the software library.

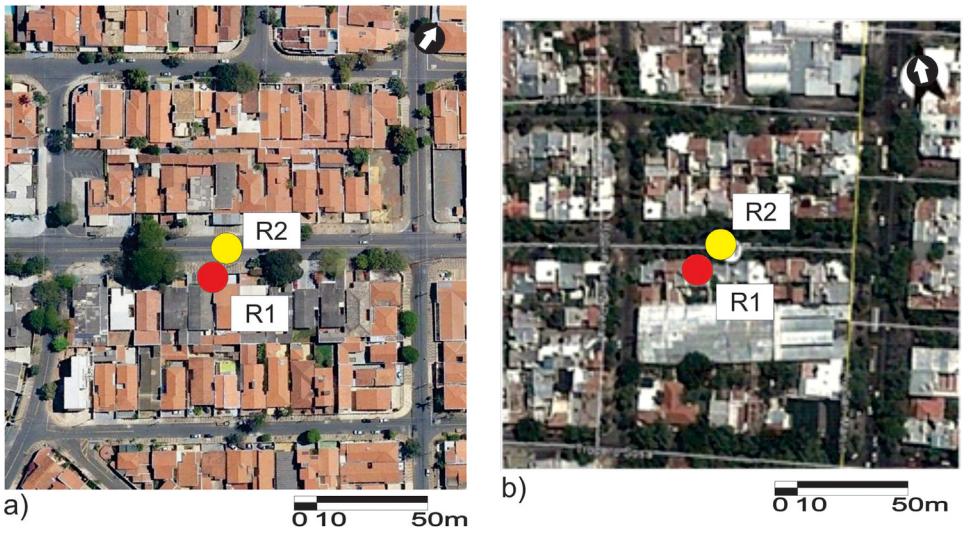

Fig. 1. Aerial images of study area of (a) Campinas and (a) Mendoza city. Monitoring point (R1) and receptor position (R 2). Source: Adapted Google Earth, 2013.

Table 2
Morpho-material features of area in Campinas (C) and Mendoza (M).

Morpho-material features	Campinas (C)	Mendoza (M)
Building height (m.)	4 to 7	4 to 9
Width of the evaluated street (meters.)	12	12
Width of the evaluated sidewalk (meters)	10	8
Forestalls height (meters)	7 to 10	10 to 15
Percentage of vegetation in urban canyons (%)	20	60 %
Built fractions (%)	47	45
H/W aspect	0.22	0.30
Sky View Factor (SVF, %)	78	45
Vehicular pathways material	concrete (albedo= 0.2)	concrete (albedo=0.3)
Pedestrian pathways material	concrete and limestone (albedo= 0.2-0.4)	limestone (albedo= 0.3-0.4)
Wall material	stones and paints in different shades (albedo= 0.2)	paints in different shades (albedo= 0.2)
Roof material	predominantly ceramic tiles and a small percentage of roofs of sheet metal and slabs concrete slab (albedo=0.3).	flat roofs of concrete slab and sloping roofs of sheet metal or ceramic tile (albedo= 0.3)
ENVI-Met models of study area	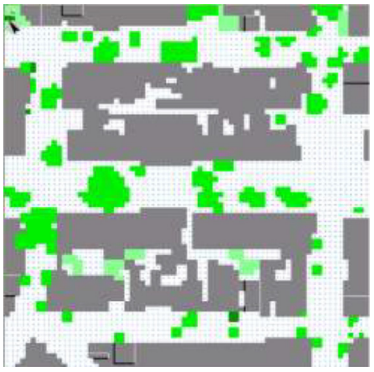	
ENVI-Met 3d models of study area	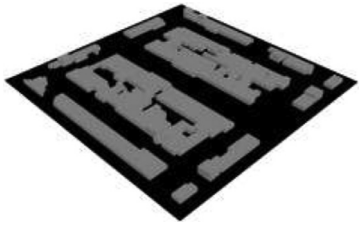	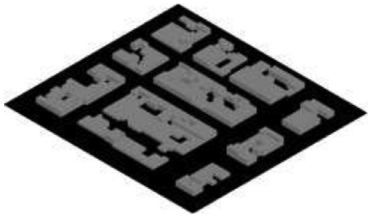

2.3. Simulation model calibration

Fig. 1 indicates the location of receptor R1, which corresponds to the monitoring and calibration point of the study area and receptor R2 which corresponds to the point where the analysis of the results was carried out in each scenario. To verify the accuracy of the model, a comparison of the air temperature curve was made between the observed and simulated data for R1 at the same sensor height in each area.

Table 4 shows the calculated statistical indices: the mean square error (RMSE) and its systematic (RMSES) and unsystematic (RMSEu) components, the deviation of the means (MBE - Mean bias error), and the coefficient of determination (R^2). There is a good fit between fixed *Point 1* and the simulated one since the R^2 values were close to 1 in both cities.

Table 3
Input parameters for ENVI-Met simulation. City of Campinas (C) and Mendoza (M).

Dates		Campinas	Mendoza
Main	Wind Speed in 10 m ab. Ground [m/s]	1.90	3.00
Data	Wind Direction (0: N; 90: E;180:S; 270: W)	135	150
	Roughness Length z0 at reference point	0.1	0.1
	Initial Temperature Atmosphere [K]	295	300
	Specific Humidity in 2500 m [g water/kg air]	8.2	2.8
	Relative Humidity in 2m [%]	66	28
Solar adjust	Factor of shortwave adjustment	1.5	1.5

Table 4
Statistical indicators of air temperature curve (°C) of the numeric model (ENVI-Met) and fixed point in both cities.

Indices	Campinas (C)	Mendoza (M)
R^2	0.97	0.99
RMSE	1.59°C	0.86°C
$RMSE_S$	1.33°C	0.52°C
$RMSE_U$	0.64°C	0.50°C
MBE	-1.03°C	0.49°C

The low magnitudes of the RMSE indicator and its RMSES and RMSEU components suggest that the simulated scenarios reflect a good fit of the microclimatic conditions observed in the study areas of both cities. The negative value of the MBE (-1.03°C) indicates that the mean value is underestimated, whereas for Mendoza it is overestimated (0.49°C). The calibration of the model was published in [9].

2.4. Study scenarios

In order to verify the potential of albedo and vegetation as strategies to mitigate urban warming, 18 different scenarios were simulated in each city. These scenarios were digitized contemplating the same area and resolution. The criterion used for the variation of the vegetation was its percentage in the urban canyon: 20% of the canyon vegetation corresponds to the actual situation of Campinas city (V_20), named 1.b; and 60% of the canyon vegetation corresponds to the actual situation of Mendoza city (V_60), named 1.a. The scenario without the presence of vegetation (V_0) was also considered. The density variable was analyzed in two scenarios: low density (L) -current situation of each city- with a H/W aspect=0.2-0.3, and high density -with a H/W aspect =1.5 (H). The albedo variation presented 3 three different scenarios with different albedo configurations low albedo, which is the current situation of the two cities (A_Low); high albedo on all surfaces of the urban envelope -streets, roofs and walls- (A_High); and combined albedo, which includes high albedo on horizontal envelope -roof, sidewalks and street- and low albedo in vertical envelope -walls- (A_Comb). These scenarios were proposed for both cities (Table 5).

Table 6 shows that the albedo parameters are similar for both cities, justifying their comparison.

In order to estimate the individual weight of each strategy and their integration on the mitigation potential of urban warming, the analyses also included the grouping of study scenarios based on the thermal difference in air temperature. This was divided into two groups: *One Strategy* and *Two Strategies*. Both groups consider scenarios with 0% Vegetation (V_0) and Low Albedo (A_Low) as a reference, as well as a scenario with low building *L* density -1.c - and *H* density -3. c. In this sense, in the *One Strategy* group an increase in vegetation from V_0 to 20 or from V_0 to 60, and an increase in albedo from A_Low to High or from A_Low to Comb will be evaluated in both low and high urban density. The *Two Strategies* group also considered scenarios 1.c and 3.c as references but with the addition of two strategies -albedo and vegetation (A + V) -, also at different densities (Table 7).

Table 5
Configuration of the 18 assessed scenarios, according to albedo variation, vegetation percentage and H/W aspect ratio.

H/W	Scenarios	Vegetation (V)	Albedo (A)
Low (L Campinas	1.a	60% *(V_60)*	Low *(A_Low)*
(C)= 0.2 Mendoza	1.b	20% *(V_20)*	Low *(A_Low)*
(M)= 0.3	1.c	0% *(V_0)*	Low *(A_Low)*
	2.a	60% *(V_60)*	High *(A_High)*
	2.b	20% *(V_20)*	High *(A_High)*
	2.c	0% *(V_0)*	High *(A_High)*
	5.a	60% *(V_60)*	Combined *(A_Comb)*
	5.b	20% *(V_20)*	Combined *(A_Comb)*
	5.c	0% *(V_0)*	Combined *(A_Comb)*
High (H) Campinas	3.a	60% *(V_60)*	Low *(A_Low)*
(C) =1.5 Mendoza	3.b	20% *(V_20)*	Low *(A_Low)*
(M)=1.5	3.c	0% *(V_0)*	Low *(A_Low)*
	4.a	60% *(V_60)*	High *(A_High)*
	4.b	20% *(V_20)*	High *(A_High)*
	4.c	0% *(V_0)*	High *(A_High)*
	6.a	60% *(V_60)*	Combined *(A_Comb)*
	6.b	20% *(V_20)*	Combined *(A_Comb)*
	6.c	0% *(V_0)*	Combined *(A_Comb)*

3. Results

In this paper, the results were structured in 3 sections:

- Descriptive analysis: Assessment of the simulation results obtained with the ENVI-Met software in the 36 proposed scenarios;
- Principal Component Analysis (PCA): Assessment to establish possible associations between the proposed mitigation strategies - vegetation and albedo - for low and high H/W scenarios
- Estimation of anthropogenic heat: Analysis of the weight of AH associated with each configuration or evaluated scenario.

3.1. Descriptive analysis

This section summarizes the simulation results of the 36 study scenarios in both cities (18 for each city) based on the output data from the receptor R2 in ENVI-Met software. Table 8 shows the daily air temperature variation at 2.1m high. The analyzed air temperature values correspond to a one-day cycle, every 30 minutes on a typical summer day. When comparing the air temperature values of each scenario, a variation from 19.0°C (Tmin in 5.a) to 34.8°C (Tmax in 1.c) in Campinas and from 21.8°C (Tmin in 5.a) to 37.3°C (Tmax in 1.c) in Mendoza is shown (Table 8).

3.2. Campinas

In the city of Campinas, the current scenario includes 20% vegetation in the urban canyon and low albedo in its urban envelope (1.b).

- In the hottest hours (daytime hours) results show that the strategy of increasing the percentage of vegetation from V_20 to V_60 presents greater efficiency among the L-density scenarios (1,2,5. b vs 1,2,5. a). These scenarios decreased their air temperature between 3.5°C and 3.9°C. In contrast, in the H-density scenarios (3,4,6. b vs 3,4,6.

Table 6
Characteristics of horizontal and vertical surfaces for the 3 Albedo Scenarios.

	Albedo (A)							
	Roofs		Walls		Predestrian pathways		Vehicular pathways	
Scenarios	C	M	C	M	C	M	C	M
Low albedo (A_Low)	0.3	0.3	0.2	0.2	0.2 - 0.4	0.3 - 0.4	0.2	0.2 - 0.3
High albedo (A_High)	0.8		0.8		0.7		0.7	
Combined albedo (A_Comb)	0.8		0.2		0.7		0.7	

Table 7
Grouping of study scenarios for thermal difference analysis.

		Low H/W (L) HW=0.2 - 0.3									Hight H/W (H) HW=1.5								
Strategies	Scenarios	1.a	1.b	1.c	2.a	2.b	2.c	5.a	5.b	5.c	3.a	3.b	3.c	4.a	4.b	4.c	6.a	6.b	6.c
One	**V_0 to 20**			*									*						
	V_0 to 60			*									*						
	A_Low to High			*									*						
	A_Low to Comb			*									*						
Two	**A+V**			*									*						

* Reference Scenarios (Low Albedo and 0% of Vegetation).

Table 8
Air temperature distribution simulated for each scenario: Median (Med), Minimum (Min) and Maximum (Max).

		Temp	Campinas		Mendoza	
	Veg %	˚C	Low H/W (L) (0.3)	High H/W (H) (1.5)	Low H/W (L) (0.2)	High H/W (H) (1.5)
Low Albedo (A_Low)	**60% (V_60)**	Med	**1.a** 22.8	**3.a** 21.9	**1.a*** 27.7	**3.a** 27.0
		Min	19.3	19.8	22.2	23.1
		Max	28.3	26.9	35.6	33.7
	20% (V_20)	Med	**1.b**** 24.9	**3.b** 23.3	**1.b** 28.7	**3.b** 27.9
		Min	20.4	20.6	22.7	23.7
		Max	32.2	29.6	36.7	34.9
	0% (V_0)	Med	**1.c** 26.4	**3.c** 24.1	**1.c** 29.2	**3.c** 28.2
		Min	21.4	21.2	22.9	23.9
		Max	34.8	31.3	37.3	35.3
High Albedo (A_High)	**60% (V_60)**	Med	**2.a** 22.4	**4.a** 23.5	**2.a** 27.1	**4.a** 27.8
		Min	19.2	20.4	22.0	23.5
		Max	27.5	29.2	34.1	34.7
	20% (V_20)	Med	**2.b** 24.2	**4.b** 24.3	**2.b** 28.2	**4.b** 28.3
		Min	20.2	21.2	22.6	23.9
		Max	30.9	31.1	35.6	35.4
	0% (V_0)	Med	**2.c** 25.6	**4.c** 24.8	**2.c** 28.6	**4.c** 28.7
		Min	21.2	21.7	22.8	24.3
		Max	33.2	32.0	36.1	35.5
Combinad Albedo (A_Comb)	**60% (V_60)**	Med	**5.a** 22.0	**6.a** 21.5	**5.a** 26.7	**6.a** 26.4
		Min	19.0	19.7	21.8	22.9
		Max	26.9	25.3	33.4	32.1
	20% (V_20)	Med	**5.b** 23.9	**6.b** 22.7	**5.b** 27.9	**6.b** 27.2
		Min	20.1	20.4	22.4	23.3
		Max	30.4	27.6	35.1	33.5
	0%(V_0)	Med	**5.c** 25.3	**6.c** 23.5	**5.c** 28.3	**6.c** 27.6
		Min	21.1	21.0	22.6	23.7
		Max	32.8	29.3	35.7	33.8

*/**Actual Scenarios: *Mendoza (1.a) and **Campinas (1.b). The scenarios that have the subscript “a” and “b”, have 2 strategies in their configuration, while scenarios with subscript “c” have “1” strategy

a), air temperature decreases from 1.9˚C to 2.7˚C. The most efficient scenario in terms of reducing maximum temperatures through the increase of vegetation was L density and low albedo (A_Low) (1.a). For example, when comparing the current scenario 1.b, 32.2˚C, with scenario 1.a, 28.3˚C, a thermal difference of 3.9˚C was obtained.

- In the coldest hours (nighttime hours) results show that the increase in vegetation from V_20 to V_60 in L (1,2,5. b vs 1,2,5. a) and H (3,4,6. b vs 3,4,6. a) densities causes a decrease between 0.7˚C and 1.1˚C. In keeping with this, when comparing scenarios 1.b to 1.a, this strategy continues to show the highest efficiency (decrease of 1.1˚C), with minimum thermal values of 20.4˚C and 19.3˚C, respectively (Table 8).

The strategy of increasing vegetation in scenarios with L and H densities for the city of Campinas offers a great advantage for cooling the urban canyon. It is important to point out that the combined albedo strategy (A_Comb)- high albedo on horizontal surfaces and low albedo for the vertical- together with the increase in vegetation presented the lowest minimum temperatures, 19.0˚C (5.a and 6.a). In addition, scenario 6.a (with H density, V_60 and A_Comb) was the most effective during maximum temperatures, 25.3˚C (Table 8).

3.3. Mendoza

In the city of Mendoza, the current scenario includes 60% of vegetation in the urban canyon and low albedo in its urban envelope (1.a).

- In the hottest hours (daytime hours), results show that the cost of reducing the vegetation from V_60 to 20 was the increase in air temperatures. This situation becomes even more critical in scenarios L

(1,2,5.a vs 1,2,5.b), with maximum temperature differences between 1.1°C and 1.7°C, in comparison with the H (3,4,6.a vs 3,4,6.b), scenarios that showed differences from 0.7°C to 1.4°C.
- In the coldest hours (nighttime hours), results show that reducing the percentage of vegetation from V_60 to V_20 in L (1,2,5.a vs 1,2,5.b) and H scenarios (3,4,6.a vs 3,4,6.b), had a lower impact, with differences around 0.4° to 0.6°C in air temperature (Table 7).

Similar to the results in the city of Campinas, in Mendoza the L density scenario with V_60 and A_Comb (5.a) was the most effective considering the minimum temperatures (21.8°C). The 6.a scenario (with H density, V_60 and A_Comb) in maximum temperatures was the most effective (32.1°C) (Table 7).

Fig. 2 describes the air temperature distribution of the 36 studied scenarios at a pedestrian's height (2.1m) at 3:00 p.m. This figure shows that the city of Mendoza registers higher air temperatures than Campinas. When analyzing the behavior in both cities, it is observed that the H scenarios remain cooler than the L ones. In fact, the maximum differences recorded are between scenarios 5.c versus 6.c, with differences of 3.5°C in Campinas and 1.9°C in Mendoza. The only exception is for scenario 2.a. which is the only *L*-density scenario cooler than its *H*-density analogy (See Table 7, 2.a vs 4.a) (Table 7).

3.3.1. Thermal performance of scenarios with one and two strategies

Fig. 3 shows the air temperature differences to identify the individual impact of each strategy in the studied scenarios. The temperature reductions concerning the reference scenarios, without mitigation strategy (1.c and 3.c), are represented with a negative sign (-). In the vast majority of the studied scenarios, the strategy of increasing vegetation has a greater impact, being greater in the city of Campinas than in Mendoza due to the physical and biological configuration of trees and the type of climate. In contrast, albedo has a more controlled effect and a similar trend in both cities, in other words, with similar geometries, the materials are expected to behave similarly. Fig. 3.a describes the temperature differences during warm-up period (ΔMax) and Fig. 3.b describes the temperature differences during cooling period (ΔMin).

3.4. One Strategy

3.4.1. Vegetation

- In the hottest hours (daytime hours) results show that the strategy of increasing vegetation in scenarios with L-density has a greater impact on the city of Campinas with reductions between -2.7°C (V_0 to 20) (1.c vs 1.b) and - 6.5°C (V_0 to 60) (1.c vs 1.a), in comparison to Mendoza where the smallest thermal variations of temperature range between -0.6°C (V_0 to 20) (1.c vs 1.b) and -1.7°C (V_0 to 60) (1.c vs 1.a). In H scenarios the cooling effect of vegetation is lower, -1.7°C (V_0 to 20) (3.c vs 3.b) and -4.3°C (V_0 to 60) (3.c vs 3.a) in Campinas and -0.4°C (V_0 to 20) (3.c vs 3.b) and -1.5°C in Mendoza (V_0 to 60) (3.c vs 3.a). It can be inferred that the cooling effect produced by the tree cover is masked by the shading effect produced by tall buildings (Table 8 and Fig. 3.a).
- In the coldest hours (nighttime hours), results show that the 60% increase in vegetation (V_0 to 60) presented the best performance, reaching a maximum reduction of -2.1°C in L-density (1.c vs 1.a) for Campinas and -0.8°C in H-density for Mendoza (3.c vs 3.a in Table 8 and Fig. 3.b).

3.4.2. Albedo

- -In the hottest hours (daytime hours), the strategy of increasing albedo has a very similar thermal performance in the two cities. In *H*, the increase in albedo (A_Low to High) tends to increase air temperature during maximum temperatures. Campinas shows a greater impact (0.7°C) than Mendoza (0.2°C) (3.c vs 4.c). This small difference can be explained by the fact that the urban canyon in Campinas is slightly more open (H/W=0.2) than Mendoza (H/W=0.30), allowing a greater access of solar radiation (Table 8 and Fig. 3.a).
- -In the coldest hours (nighttime hours), it is also verified that in scenarios where the albedo value has been increased (A_Low to High) air temperatures become higher in both cities, contributing to the formation of the heat island in the scenarios with *H*. Air temperature registered increases of 0.6°C in Campinas and 0.4°C in Mendoza (3.c vs 4.c). That is, the strategy of increasing the albedo on all surfaces favors the formation of a high-density heat island (*H*) [14] (Table 8 and Fig. 3.a).

The scenarios with A_Comb - higher albedo on horizontal surfaces and lower on vertical ones - have the best performance in both the maximum and minimum temperature occurrence period, for *L* (5) and *H* density (6). Thermal reductions of -1.6°C to -2.0°C (*L*) and -1.5°C to -2.0°C (*H*) during the hottest hours of the day can be observed for Mendoza and Campinas respectively (Fig. 3.a). Both cities also show -0.3°C (*L*) and -0.2°C (*H*) during the minimum temperatures (Fig. 3.b).

3.5. Two strategies

This section analyses the thermal performance of *L* and *H* density scenarios for the minimum and maximum temperature considering the two integrated strategies, *-Two strategy:* increase in vegetation and albedo- (Fig. 4).

- In the hottest hours (daytime hours), there were greater decreases in temperature than during coldest hours, as for the case in the -*One strategy*- scenarios. During maximum temperature, the scenarios registered maximum temperature reductions of up to -7.9°C in Campinas and -3.8°C in Mendoza (1.c vs 5.a in Table 8 and Fig. 4).
- In the coldest hours (nighttime hours), the performance with -*Two strategies*- is more efficient than the one with -*One strategy*- in both cities, reaching a minimum temperature reduction up to -2.3°C in Campinas and 1.1°C in Mendoza (1.c vs 5.a in Table 8 and Fig. 4).

The thermal benefit of the combined strategies in Campinas coincides with that reported by [10]. It is observed that the integration of two or more mitigation technologies provides a lower contribution than the theoretical sum of the individual effects since the albedo and vegetation strategies are in part complementary and in part overlapping. However, in the case of the city of Mendoza, it is verified that the combination of both strategies slightly (0.5°C) enhances the thermal benefit of their implementation (Figs. 3.a and 4).

3.6. Principal components analysis (PCA)

In this section, the Principal Component Analysis (PCA) was carried out in order to evaluate the possible associations between the variables. For this research, the correlation matrix that works with variables measured in different units was used [69]. For the realization of the PCA, air temperature data were collected in a matrix every 30 minutes of a measurement day of all the 36 study scenarios together with the tabulation of the following variables: sky view factor (SVF), weighted albedo (Aw) and percentage of Vegetation (V). The weighted albedo (*Aw*) included the weighted average of the albedo of roofs, façades, vehicular and pedestrian pavements. The *Aw* was calculated by adding the areas of all the surfaces in the study area multiplied by the albedo value of each surface.

The use of subgroups from several variables is recommending, when among themselves does not promote significant changes in the results [70,71]. In this study, PCA contemplated individual analyzes of each study city in L and H urban density.

Tables 9 and 10 and Fig. 5 present the results of a two-component model which evidences a good representation of the studied data, showing that the behavior of air temperature within the urban channel can be explained by two main factors. The model showed a good representation considering that variances greater than 70% are represented in the first and second components. Both in high (*H*) and in low density (*L*)

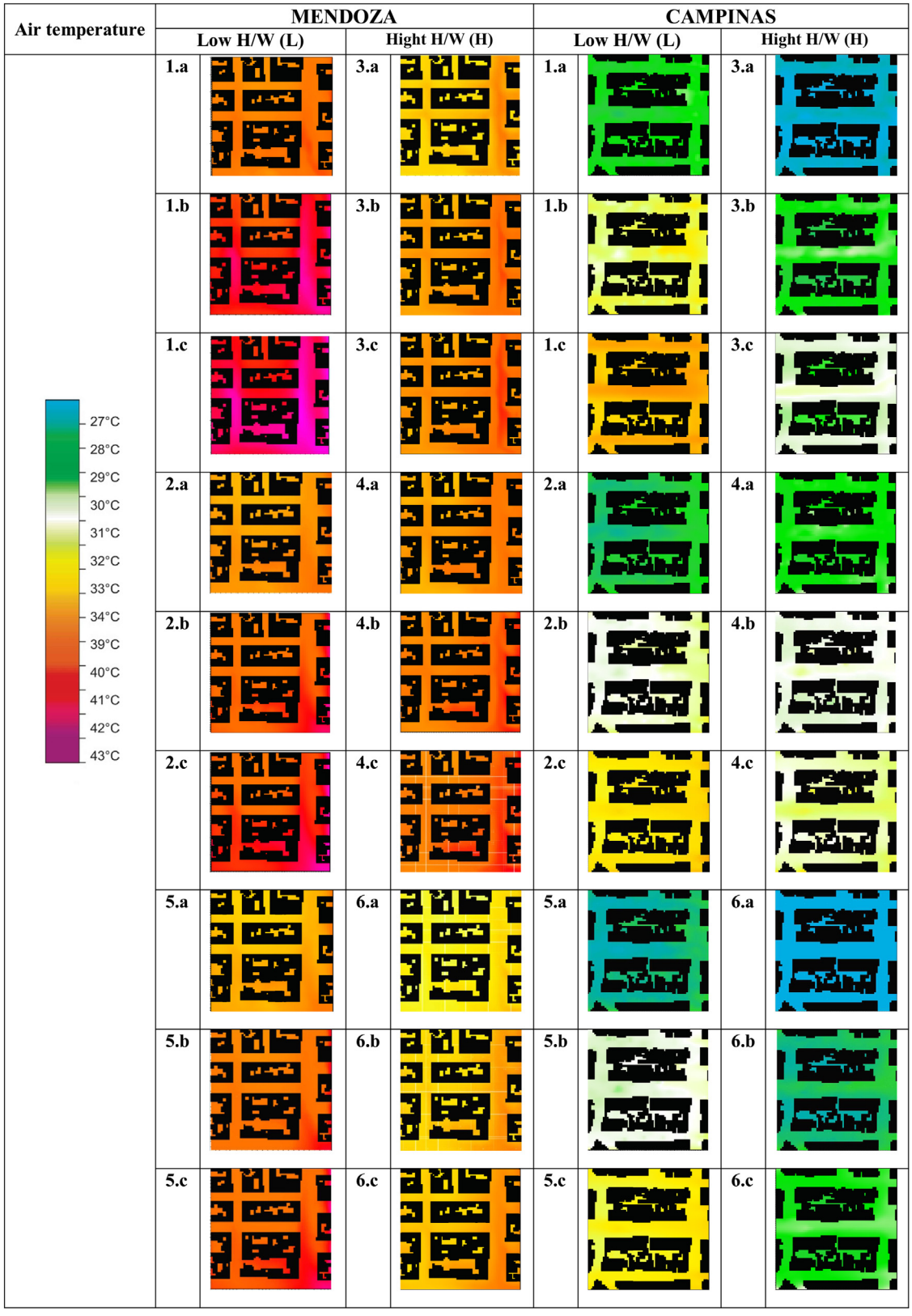

Fig. 2. ENVI-Met outputs rendered in LEONARDO of 36 scenarios analyzed, 15:00 hours, at pedestrian's height.

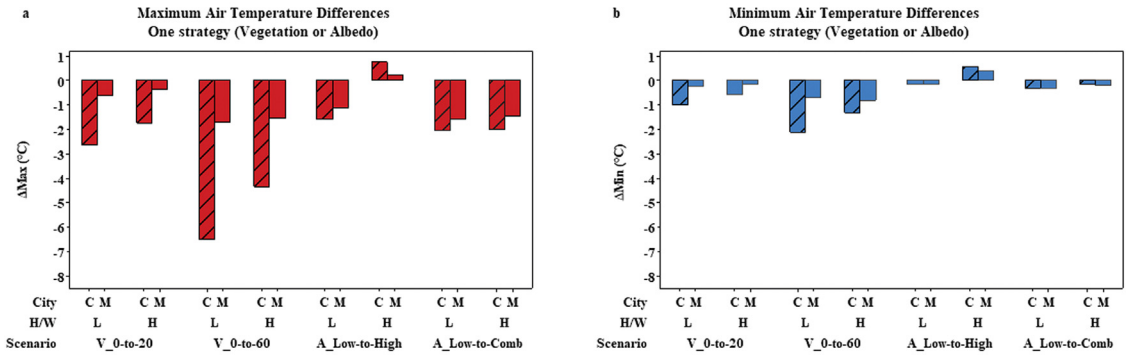

Fig. 3. Air temperature differences for *One Strategy* (vegetation or albedo) according to the reference scenarios (1c - Low H/D and 3c - High H/W). (a) Maximum (b) Minimum.

Table 9
Principal Component Analysis – Eigen analysis of the Correlation Matrix. Low and High H/W study scenarios.

Correlation Matrix	Campinas Low H/W				Mendoza			
	PC1	PC2	PC3	PC4	PC1	PC2	PC3	PC4
Eigenvalue	2.225	1.024	0.719	0.030	1.995	1.061	0.900	0.042
Proportion	0.556	0.256	0.180	0.008	0.499	0.265	0.225	0.011
Cumulative	0.556	**0.812**	0.992	1.000	0.499	**0.764**	0.989	1.000
	High H/W							
	PC1	**PC2**	**PC3**	**PC4**	**PC1**	**PC2**	**PC3**	**PC4**
Eigenvalue	1.9910	1.0754	0.7797	0.1539	1.9774	1.0127	0.9597	0.0502
Proportion	0.498	0.269	0.195	0.038	0.494	0.253	0.240	0.013
Cumulative	0.498	**0.767**	0.962	1.000	0.494	**0.748**	0.987	1.000

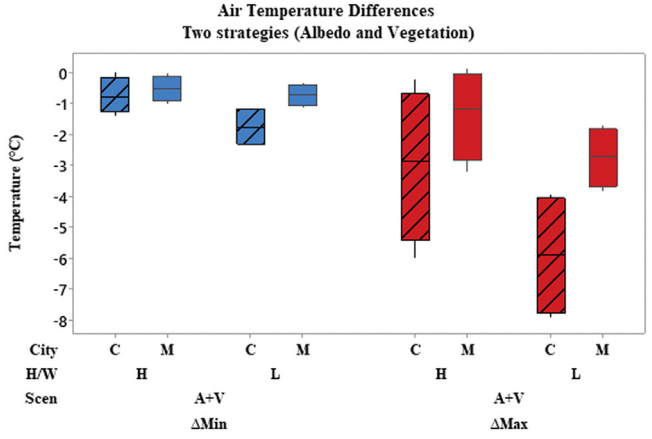

Fig. 4. Boxplot of air temperature differences for two strategies (albedo and vegetation) according to the reference scenarios (1c - Low H/D and 3c - High H/W). Maximum and Minimum.

Table 10
Values of the study variables in relation to the first and second Principal Component. Low and High H/W study scenarios.

Variable	Campinas Low H/W		Mendoza	
	PC1	**PC2**	**PC1**	**PC2**
Weighted Albedo (Aw)	0.032	**-0.957**	0.016	**-0.787**
Vegetation (V)	**0.643**	0.105	**0.694**	0.092
Sky View Factor (SVF)	**-0.642**	-0.105	**-0.693**	-0.094
Air Temperature (T)	-0.416	0.251	-0.194	0.603
	High H/W			
	PC1	**PC2**	**PC1**	**PC2**
Weighted Albedo (Aw)	0.051	**0.857**	0.004	**-0.872**
Vegetation (V)	**-0.662**	0.152	**-0.698**	-0.059
Sky View Factor (SVF)	**0.655**	-0.168	0.697	0.061
Air Temperature (T)	0.361	0.463	0.166	-0.482

there is a good representation, 81.2% and 76.4% of the total variance in *L* (Fig. 5.a, b), and 76.7% and 74.8% in *H* (Fig. 5.c, d), in Campinas and Mendoza, respectively.

Table 9 shows the contribution of each variable in the formation of components. The highlighted values are those with a significance close to 0.7. When considering air temperature as a dependent variable, the most significant variables are V and SVF in the first component (PC1) and Aw, in *L* and *H* in the second component (PC2). In *L* density for both cities, the SVF is inversely related to V (Table 10). Therefore, as the ratio of V increases, SVF and temperature decrease and vice versa. PC2 is represented by *Aw*, where air temperature is inversely related to this variable, that is, an *Aw* increase in areas of *L* provides a decrease in air temperature, and vice versa.

In addition, this is in accordance with the results of the simulation where the strategies of increasing V and *Aw* in low density are efficient for both cities. In high density for both cities, SVF in PC1 is also inversely related to V. Therefore, as the proportion of V increases, SVF and temperature decrease. In PC2, the air temperature is directly related to the *Aw* of the surfaces, therefore, as the weighted albedo increases, the air temperature increases.

3.7. Estimation of anthropogenic heat

In this work, the efficiency of the application of different urban retrofitting strategies to mitigate overheating of cities has been discussed. The described results show that in both *L* and *H* urban density conditions, it is possible to obtain improvements in the thermal response of the urban canyon through the implementation of the evaluated strategies. This could even lead to think that an increase in the aspect of the H/W ratio could be an efficient alternative to reduce air temperatures due to the effect of the shadows produced by building height (Fig. 4). However, to fully measure the effect of urban densification in combination with the evaluated strategies, it is necessary to include the effect of the increase in anthropogenic contribution associated with the inten-

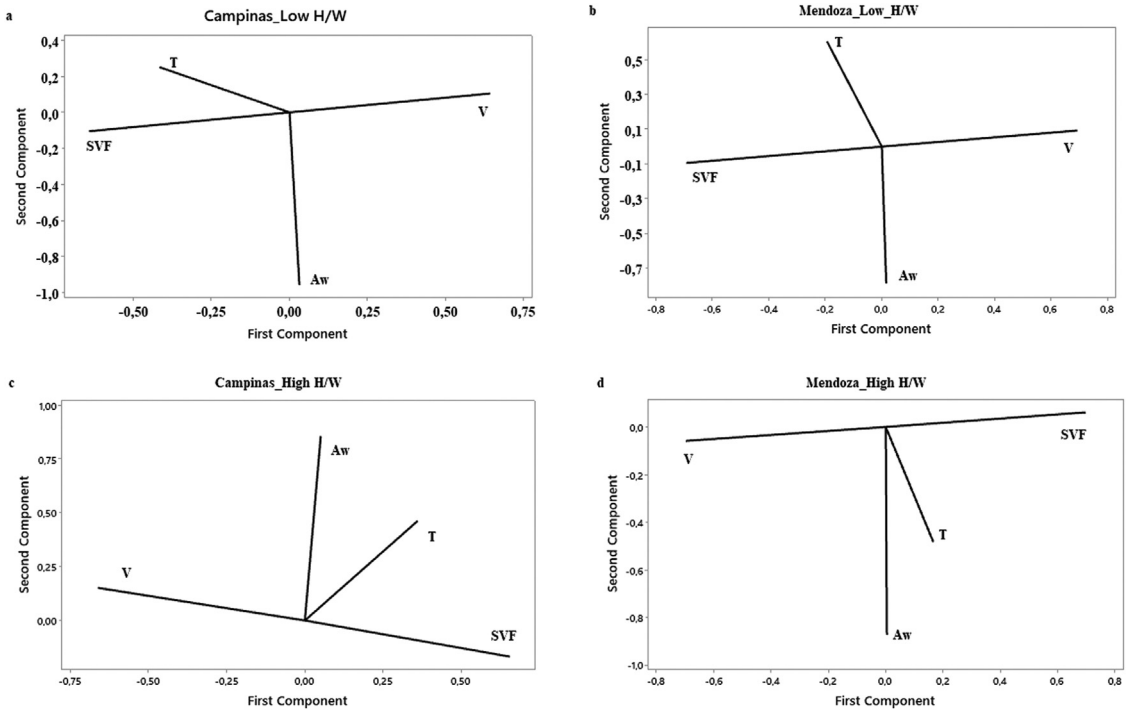

Fig. 5. Principal Component Analysis: Albedo (Aw). Vegetation (V). Sky View Factor (SVF). Air Temperature (T). (a) and (b) Low H/W. (c) and (d) High H/W.

sification in the use of urban land in the theoretical simulation model. Despite the fact that the ENVI-Met software is one of the most robust tools to predict the local microclimate, it does not consider the AH - sensitive and latent- per unit area caused by the increase in the H/W aspect (*L* to *H*). For this reason, this section seeks to estimate the weight of the anthropogenic variable on air temperature and improve the results of the ENVI-Met simulations by using the Urban Weather Generator (UWG) model.

The UWG was developed by Bruno Bueno at the Massachusetts Institute of Technology as a fast-numerical solver for simulating the urban microclimate environment, taking into account the rural climate, the urban building characteristics and the AH in the urban area [72]. The UWG software considers a building energy model that includes the heat load of the occupants and assumes that non-building AH consists only of traffic heat [73].

To estimate the contribution of AH in the analyzed cities, a reference value of 4.5 W/m^2 was considered in scenarios with low H/W (*L*) for the sensitive AH peak. In scenarios with high H/W (*H*), values were established as follows: 0.5 W/m^2 for the latent AH peak, 15 W/m^2 for the sensitive AH peak and 1.5 W/m^2 for the latent AH peak. These values are based on the literature of Afshari; Schuch; and Marpu [74] and Quah and Roth [75].

Fig. 6 shows the differences in air temperatures (for minimum and maximum temperature cases), resulting from densifying the scenarios from low to high density, going from a radio aspect of 0.2 to 1.5 in Campinas and 0.3 to 1.5 in Mendoza. The figure shows the impact of densification in grey and the impact of the increase in AH on air temperature in red or blue for each of the evaluated cases in both cities.

- In the hottest hours (daytime hours), it is observed that the greatest impact of anthropogenic loads coincides with the period of greatest anthropic flow. These charges raise the temperature of the scenarios to 1.6°C and 1.2°C in Campinas and Mendoza, respectively. In this period, it is verified that the effect of densifying decreases air temperature for most of the scenarios analyzed in a range of 0.2°C to 3.5°C. However, it is observed that when the effect of the building shade is greater, the thermal loads produced by AH in high-density scenarios can decrease and even cancel or impair the thermal response of the analyzed urban canyon. See for example the cases 6c vs 5.c in Campinas and Mendoza where the thermal benefit is reduced, and the cases of 4.c vs 2.c, where the benefit is cancelled or lowered (Fig. 6).
- In the coldest hours (nighttime hours), it was observed that the incorporation of AH in the *H* scenarios produces increases in the minimum air temperature of 0.5°C in both cities. In other words, when considering the effect of AH in the *H* scenarios, the existing UHI generation is further damaged. Minimum air temperature increases up to 1.5°C (4.c vs. 2.c) were recorded (Fig. 6).

It should be noted that the heat from traffic is much lower than other heat sources such as sensible heat from the street, the wall, and residual heat from buildings [73].

4. Discussion and conclusions

This section has been prepared based on the thematic axes explored in this research: Effects of cooling technologies over the microclimate of low and high building densities of urban spaces and the impact of human-processes in urban modelling. The results reinforce the beneficial effect of vegetation strategies and increased albedo (high or combined) on city surfaces to mitigate urban warming. However, the performance of isolated and/or integrated strategies depends on building density, the analyzed period, and the climate. The results of 36 scenarios in different climates integrating different mitigation strategies allowed us to reach the following conclusions:

a The increase in vegetation from V_0 to 20 and from V_0 to 60 has a high impact on both climates analyzed, despite the different behaviors shown in both cities. This difference can be explained by the characteristics of the vegetation and the type of climate where it is inserted. The greatest impact was during the maximum low-density temperature (*L*), a reduction of -2.7° and -6.5°C in Campinas (Cwa) and of -0.6° and -1.7°C in Mendoza (BWh). This shows that the effect of tree shadows has a positive impact. In high-density (*H*) the effect was lower but representative, -1.7°C and -4.3°C in Campinas

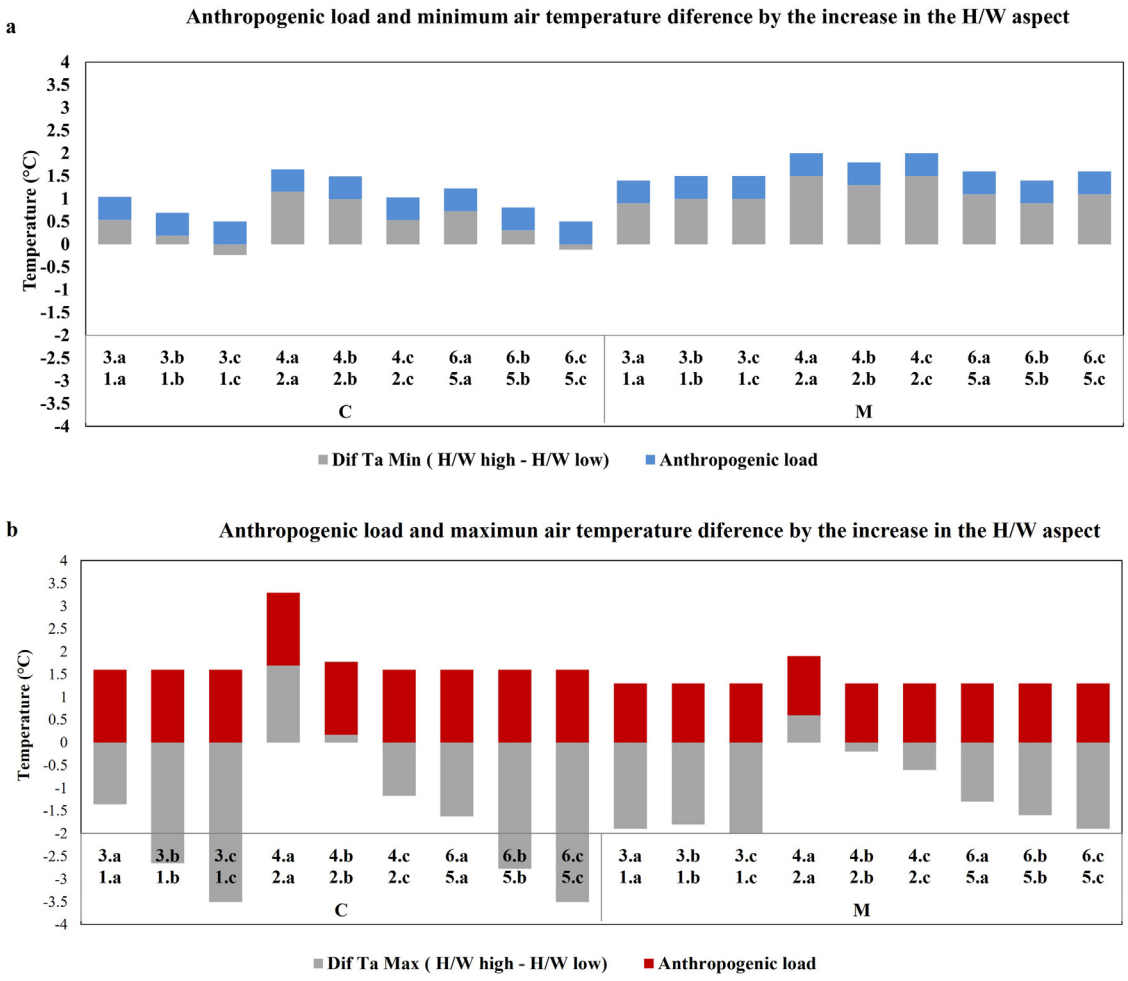

Fig. 6. Simulated air temperature difference (Dif Ta) between H/W high (H) and H/W low (L) scenarios. Highlighting air temperature differences plus by the anthropogenic load. (a) Minimum. (b) Maximum.

and -0.4˚C and -1.5˚C in Mendoza. In these cases, it can be inferred that the cooling effect produced by the canopy tree is masked by the effect of shadows cast by tall buildings. In the cooling period, the best performance was in low-density (*L*), with a reduced range of -0.2˚C to -2.1˚C.

b The strategy of increasing the albedo on horizontal and vertical surfaces intensified the heat island effect in high-density (H), for both cities. The results showed an increase in the maximum temperature up to 0.7˚ and up to 0.6˚C for the minimum temperature. These results can be explained by the building height effect and the reflective materials which cause multiple reflections that increase the radiation absorption, consequently contributing to an increase of the temperature of the urban canyon at a rate of 1.7˚C in Campinas and 0.6˚C in Mendoza. That is, the strategy of increasing the albedo on all surfaces favors the formation of UHI in scenarios with a high-density (*H*). These results are in keeping with the reported by Alchapar et. al. [23], and Pisello [24].

c The combined albedo strategy (A_Comb) – high on horizontal surfaces and low on vertical surfaces - is efficient in both low and high density and can reduce air temperature up to 2.0˚C, showing a better performance during peak hours. We verified that the strategy to increase the albedo led to a similar behavior in both cities, in other words, with similar geometries, materials are expected to present a similar performance.

d Integrated strategies have the potential to mitigate urban warming, with a greater impact at low-density. The results showed that in low density (*L*) there was an average reduction -more frequent value- of the maximum air temperature of 5.9˚C and 2.7˚C in the daytime period; and 1.8˚C and 0.7˚C in the nocturnal period in Campinas and Mendoza, respectively. Although this impact is lower in high-density (*H*), results are promising with a mean reduction of the maximum air temperature of 2.9˚C and 1.2˚C in the daytime period; and of 0.8˚C and 0.5˚C in the night period. It is also observed that the integration of two strategies does not enhance the formation of the nocturnal heat island, a behavior that can be evidenced when albedo is increased on all surfaces.

To summarize, the strategies to increase the vegetation and the albedo of urban surfaces can strongly contribute to mitigate urban warming. In addition, they promote the improvement of thermal comfort in the open urban space.

Based on statistical analyses, it is concluded that the strategy of increasing the albedo in high densities must be adopted with criteria. When evaluating the results of the PCA, it is verified that the variables with high weight in the PC1 component are vegetation and the sky factor, which represent the morphological aspects of each city. In PC2, the weighted albedo variable represents the technological component. Both the morphological and technological components have different behaviors at low and high densities. Vegetation, however, is efficient at different densities. Increasing the albedo on all surfaces, on the contrary, causes overheating problems in high density urban areas.

In PC2, the weighted albedo variable can be represented as a technological component. In this sense, both the morphological and technolog-

ical components have different behaviors at low and high densities. That is, vegetation is efficient at different densities, but increasing albedo on all surfaces, without distinguishing density, can cause overheating problems in urban areas. These findings are in line with those observed by Yang et al. [15].

We observe that the results obtained in the simulation were consistent with what was indicated in the Multivariate Analysis of Principal Components. The results showed that vegetation is efficient at different densities. The paradigm of increasing albedo in all urban areas without distinguishing density, orientation, or relative position of the surface - floor, roof, and facade- can cause overheating problems in the urban canyon. In contrast, increasing the albedo on horizontal surfaces is a promising strategy

The results indicated that the anthropogenic heat mainly produced by motorized transport and air conditioning systems is a crucial input data for the urban microclimate models because its impact on the urban densification processes may cancel out the benefits of the application of cooling strategies in some cases.

In addition, this work proposes the integration of the potential of ENVI-Met for microclimatic forecasting and the Urban Weather Generator software. This tool considers the anthropogenic vehicular and building heat fluxes in its calculation engine. The results are promising since it was shown that high-density AH can reduce or even nullify the beneficial effects of the application of urban cooling strategies such as albedo and vegetation for the two analyzed cities. Due to the effect of AH, increases in air temperature of up to 1.6°C in Campinas and 1.2°C in Mendoza were found during the maximum temperature peak. These results are in sound (magnitude) with those found in the international literature; Ichinose et al. [35] found that HA emissions increased the intensity of the heat island by between 1 and 1.5 °C in Tokyo. Fan and Sailor [36] showed that HA emissions in Philadelphia can cause the intensity of the heat island to increase by 2 to 3 °C on a winter night. Kusaka and Kimura [76] also found that the impact of anthropogenic warming on the nocturnal heat island is the largest of all factors in Tokyo.

Finally, this research showed that there is no optimal strategy to mitigate urban overheating. Urban planners should be aware of the different impacts these strategies have and their application must be analyzed according to the local climatic, morphological, and technological context.

Acknowledgment

This work was supported by the National Agency for Scientific and Technological Promotion-ANPCyT- of Argentina, through the Fund for Scientific and Technological Research -FONCyT (PICT2017-3248 and PICT2018-2080) and the State of São Paulo Research Foundation – FAPESP (2019/10308-9).

References

[1] E. Chatzinikolaou, C. Chalkias, E. Dimopoulou, Urban microclimate improvement using ENVI-met climate model, Int. Arch. Photogramm. Remote Sens. Spat. Inf. Sci. - ISPRS Arch. 42 (4) (2018) 69–76.
[2] M. Meinshausen, et al., Greenhouse-gas emission targets for limiting global warming to 2°C, Nature 458 (April, 2009).
[3] M. Collins et al., "Long-term Climate Change: Projections, Commitments and Irreversibility," 2013.
[4] T.R. Oke, The energetic basis of the urban heat island, Q. J. R. Meteorol. Soc. 108 (445) (1982) 1–24.
[5] M. Santamouris, Recent progress on urban overheating and heat island research . Integrated assessment of the energy, environmental, vulnerability and health impact . Synergies with the global climate change, Ennergy Build. 207 (2020).
[6] A. Baniassadi, D.J. Sailor, P.J. Crank, G.A. Ban-Weiss, Direct and indirect effects of high-albedo roofs on energy consumption and thermal comfort of residential buildings, Energy Build. 178 (Nov. 2018) 71–83.
[7] M. Santamouris, Energy and Climate in the Urban Built Environment, 1st Editi, Routledge Taylor & Francis Group, London, 2013.
[8] H. Akbari, D. Kolokotsa, Three decades of urban heat islands and mitigation technologies research, Energy Build. 133 (2016) 834–842.
[9] N.L. Alchapar, C.C. Pezzuto, E.N. Correa, L. Chebel Labaki, The impact of different cooling strategies on urban air temperatures: the cases of Campinas, Brazil and Mendoza, Argentina, Theor. Appl. Climatol. 130 (1) (2017) 35–50 –2.
[10] M. Santamouris, et al., Passive and active cooling for the outdoor built environment – analysis and assessment of the cooling potential of mitigation technologies using performance data from 220 large scale projects, Sol. Energy 154 (2017) 14–33.
[11] D. Lai, W. Liu, T. Gan, K. Liu, Q. Chen, A review of mitigating strategies to improve the thermal environment and thermal comfort in urban outdoor spaces, Sci. Total Environ. 661 (2019) 337–353.
[12] M. Thornbush, O. Golubchikov, S. Bouzarovski, Sustainable cities targeted by combined mitigation-adaptation efforts for future-proofing, Sustain. Cities Soc. 9 (2013) 1–9.
[13] G. Virk, A. Jansz, A. Mavrogianni, A. Mylona, J. Stocker, M. Davies, Microclimatic effects of green and cool roofs in London and their impacts on energy use for a typical office building, Energy Build. 88 (2015) 214–228.
[14] M. Santamouris, Cooling the cities - A review of reflective and green roof mitigation technologies to fight heat island and improve comfort in urban environments, Sol. Energy 103 (2014) 682–703.
[15] J. Yang, Z.H. Wang, K.E. Kaloush, Environmental impacts of reflective materials: Is high albedo a 'silver bullet' for mitigating urban heat island? Renew. Sustain. Energy Rev. 47 (2015) 830–843.
[16] M. Santamouris, A. Synnefa, T. Karlessi, Using advanced cool materials in the urban built environment to mitigate heat islands and improve thermal comfort conditions, Sol. Energy 85 (12) (2011) 3085–3102.
[17] A. Middel, N. Chhetri, R. Quay, Urban forestry and cool roofs: Assessment of heat mitigation strategies in Phoenix residential neighborhoods, Urban For. Urban Green. 14 (1) (2015) 178–186.
[18] F. Rosso, et al., On the impact of innovative materials on outdoor thermal comfort of pedestrians in historical urban canyons, Renew. Energy 118 (2018) 825–839.
[19] N. Alchapar, M. Sánchez Amono, E. Correa, R. Gaggino, M. Positieri, Energy-efficient urban buildings. Thermo-physical characteristics of traditional and recycled roofing technologies, Rev. Ing. Constr. 35 (1) (2020) 73–83.
[20] L.P. Muniz-Gäal, C.C. Pezzuto, M.F.H. de Carvalho, L.T.M. Mota, Eficiência térmica de materiais de cobertura, Ambient. Construído 18 (1) (2018) 503–518.
[21] N.L. Alchapar, E.N. Correa, M.A. Cantón, Classification of building materials used in the urban envelopes according to their capacity for mitigation of the urban heat island in semiarid zones, Energy Build 69 (2014) 22–32.
[22] M. Taleghani, Outdoor thermal comfort by different heat mitigation strategies - a review, Renew. Sustain. Energy Rev. 81 (2018) 2011–2018 March 2017.
[23] N.L. Alchapar, E.N. Correa, The use of reflective materials as a strategy for urban cooling in an arid 'OASIS' city, Sustain. Cities Soc. 27 (2016) 1–14.
[24] A.L. Pisello, J.E. Taylor, X. Xu, F. Cotana, Inter-building effect: Simulating the impact of a network of buildings on the accuracy of building energy performance predictions, Build. Environ. 58 (2012) 37–45 December 2012.
[25] L.V. Abreu-Harbich, L.C. Labaki, A. Matzarakis, Effect of tree planting design and tree species on human thermal comfort in the tropics, Landsc. Urban Plan. 138 (2015) 99–109.
[26] M..A. Ruiz, E.N. Correa, Esquemas urbano-forestales en una «ciudad oasis» de zona árida: Mendoza (Argentina), Inf. la Construcción 70 (549) (2018) 239.
[27] G.E. Kyriakodis, M. Santamouris, Using reflective pavements to mitigate urban heat island in warm climates - Results from a large scale urban mitigation project, Urban Clim 24 (2018) 326–339.
[28] E. Di, M. Pergolini, F. Stazi, E. Di Giuseppe, M. Pergolini, F. Stazi, Numerical assessment of the impact of roof reflectivity and building envelope thermal transmittance on the UHI effect envelope thermal transmittance on the UHI effect, Procedia Eng. 134 (2017) (2017) 404–413.
[29] S. Tsoka, A. Tsikaloudaki, T. Theodosiou, Analyzing the ENVI-met microclimate model's performance and assessing cool materials and urban vegetation applications–A review, Sustain. Cities Soc. 43 (2018) 55–76 July.
[30] M.A. Ruiz, M.B. Sosa, E.N. Correa, M.A. Cantón, Design tool to improve daytime thermal comfort and nighttime cooling of urban canyons, Landsc. Urban Plan. 167 (2017) 249–256 June.
[31] N. Chrysoulakis, C.S.B. Grimmond, Understanding and reducing the anthropogenic heat emission, Urban Clim. Mitig. Tech. (2016) 27–40.
[32] E.N. Bondank, M.V. Chester, B.L. Ruddell, Water Distribution System Failure Risks with Increasing Temperatures, Environ. Sci. Technol. 52 (17) (2018) 9605–9614.
[33] D. Burillo, M.V Chester, S. Pincetl, E. Fournier, Electricity infrastructure vulnerabilities due to long-term growth and extreme heat from climate change in Los Angeles County, Energy Policy 128 (2019) 943–953 February.
[34] R.S. Kovats, S. Hajat, Heat stress and public health: A critical review, Annu. Rev. Public Health 29 (2008) 41–55.
[35] T. Ichinose, K. Shimodozono, K. Hanaki, Impact of anthropogenic heat on urban cimate in Tokyo, Atmos. Environ. 33 (1999) 3897–3909.
[36] H. Fan, D.J. Sailor, Modeling the impacts of anthropogenic heating on the urban climate of Philadelphia: A comparison of implementations in two PBL schemes, Atmos. Environ. 39 (1) (2005) 73–84.
[37] M.G. Flanner, Integrating anthropogenic heat flux with global climate models, Geophys. Res. Lett. 36 (2) (2009) 1–5.
[38] D. Lee, C. Ferguson, R. Mitchell, Air pollution and health in Scotland: a multicity study, Biostatistics 10 (3) (2009) 409–423.
[39] A. Krpo, F. Salamanca, A. Martilli, A. Clappier, On the impact of anthropogenic heat fluxes on the urban boundary layer: A two-dimensional numerical study, Boundary-Layer Meteorol 136 (1) (2010) 105–127.
[40] R. Liu, Z. Han, The Effects of Anthropogenic Heat Release on Urban Meteorology and Implication for Haze Pollution in the Beijing-Tianjin-Hebei Region, Adv. Meteorol. 2016 (2016).
[41] L. Chen, M. Zhang, J. Zhu, Y. Wang, A. Skorokhod, Modeling Impacts of Urbanization and Urban Heat Island Mitigation on Boundary Layer Meteorology and Air Quality in

Beijing Under Different Weather Conditions, J. Geophys. Res. Atmos. 123 (8) (2018) 4323–4344.
[42] D.J. Sailor, L. Lu, A top-down methodology for developing diurnal and seasonal anthropogenic heating profiles for urban areas, Atmos. Environ. 38 (17) (2004) 2737–2748.
[43] L. Allen, F. Lindberg, C.S.B. Grimmond, Global to city scale urban anthropogenic heat flux: Model and variability, Int. J. Climatol. 31 (13) (2011) 1990–2005.
[44] M. Iamarino, S. Beevers, C.S.B. Grimmond, High-resolution (space, time) anthropogenic heat emissions: London 1970-2025, Int. J. Climatol. 32 (11) (2012) 1754–1767.
[45] S.H. Lee, C.K. Song, J.J. Baik, S.U. Park, Estimation of anthropogenic heat emission in the Gyeong-In region of Korea, Theor. Appl. Climatol. 96 (3) (2009) 291–303 –4.
[46] C. Smith, S. Lindley, G. Levermore, Estimating spatial and temporal patterns of urban anthropogenic heat fluxes for UK cities: The case of Manchester, Theor. Appl. Climatol. 98 (1) (2009) 19–35 –2.
[47] J.E. González, et al., Urban climate and resiliency: A synthesis report of state of the art and future research directions, Urban Clim 38 (2021) May.
[48] V. Masson, A. Lemonsu, J. Voogt, The 9th International Conference on Urban Climate, Urban Clim. 23 (2018) 1–7.
[49] X. Xu, et al., Using WRF-Uran to assess summertime air conditioning electric loads and their impacts on urban weather in Beijing, Geophys. Res. Atmos. 123 (2018) 2475–2490.
[50] I. Capel-Timms, C. S. B. Grimmond, S. T. Smith, and A. M. Gabbey, "An agent-based model to capture dynamics of Anthopogenic heat flux," in *10th International Conference on Urban Climate*, 2018.
[51] P.A. Mirzaei, F. Haghighat, Approaches to study Urban Heat Island e Abilities and limitations, Build. Environ. 45 (10) (2010) 2192–2201.
[52] K.C. Sáez, Impacto de las islas térmicas o islas de calor urbano, en el ambiente y la salud humana, Terra 27 (42) (2011) 95–122.
[53] P. Sarricolea, O. Meseguer-Ruiz, Urban Climates of Large Cities: Comparison of the Urban Heat Island Effect in Latin America BT, in: C. Henríquez, H. Romero (Eds.), Urban Climates in Latin America, Cham: Springer International Publishing, 2019, pp. 17–32.
[54] E. N. Correa, "Isla de calor urbana. El caso del área metropolitana de Mendoza," UNSA, Salta, Argentina, 2006.
[55] C. C. Pezzuto, "Avaliação do Ambiente Térmico Nos Espaços Urbanos Abertos. Estudo de Caso em Campinas, SP," Universidade Estadual de Campinas, 2007.
[56] M. R. C. Soeira, "A relação entre o fator de visão do céu e a temperatura do ar em diferentes Zonas Climáticas Locais," p. 116, 2018.
[57] P D. United Nations, Department of Economic and Social Affairs, The World 's Cities in 2018 - The World's Cities in 2018 Data Booklet (ST/ESA/SER.A/417), 2018.
[58] M. Kottek, Jurgen Grieser, C. Beck, B. Rudolf, F. Rubel, World Map of the Köppen-Geiger climate classification updated, Meteorol. Zeitschrift 3 (3) (2006) 259–263.
[59] IBGE, "Banco de dados Cidades: Informações sobre Municípios Brasileiros. Instituto Brasileiro de Geografia e Estatística," 2022. [Online]. Available: https://www.ibge.gov.br/cidades-e-estados/sp/campinas.html. [Accessed: 06-Apr-2022].
[60] Instituto Nacional de Estadística y Censos de la República Argentina (INDEC), "Censo Nacional de Población, Hogares y Viviendas 2001 y 2010," 2010
[61] M.F. Colli, É.N. Correa, C.F. Martinez, Aplicación del método Wudapt en la ciudad de Mendoza-Argentina para definir zonas climáticas locales, Rev. Urbano 42 (2020) 18–31.
[62] M. Bruse, H. Fleer, Simulating surface–plant–air interactions inside urban environments with a three dimensional numerical model, Environ. Model. Softw. 13 (3) (1998) 373–384 –4.
[63] L. P. Muniz-Gaal, Cláudia Cotrim Pezzuto, M. F. H. de Carvalho, and L. T. M. Mota, "Urban geometry and the microclimate of street canyons in tropical climate," Building and Environmentvol. 169, no. November2019, 2020. https://doi.org/10.1016/j.buildenv.2019.106547
[64] S. Tsoka, A. Tsikaloudaki, T. Theodosiou, Analyzing the ENVI-met microclimate model's performance and assessing cool materials and urban vegetation applications–A review, Sustain. Cities Soc. 43 (2018) 55–76 April.
[65] S. Huttner, M. Bruse, P. Dostal, Using ENVI-met to simulate the impact of global warming on the mi- croclimate in central European cities, 5th Japanese-German Meet. Urban Climatol. 18 (18) (2008) 307–312.
[66] X. Yang, L. Zhao, M. Bruse, Q. Meng, Evaluation of a microclimate model for predicting the thermal behavior of different ground surfaces, Build. Environ. 60 (2013) 93–104.
[67] M. Roth, V.H. Lim, Evaluation of canopy-layer air and mean radiant temperature simulations by a microclimate model over a tropical residential neighbourhood, Build. Environ. 112 (2017) 177–189.
[68] ENVI-met, "ENVI-met 3.1 Manual Contents," 2015.
[69] D.S. Wilks, Statistical Methods in the Atmospheric Sciences, 2nd ed., Elsevier, 2006.
[70] I.T. Jolliffe, Discarding Variables in a Principal Component Analysis . I : Artificial Data, J. R. Stat. Soc. Ser. C (Applied Stat. 21 (2) (1972) 160–173.
[71] I.T. Jolliffe, Discarding Variables in a Principal Component Analysis. II : Real Data, J. R. Stat. Soc. Ser. C (Appl. Stat.) 22 (1) (1973) 21–31.
[72] B. Bueno, L. Norford, J. Hidalgo, G. Pigeon, The urban weather generator, J. Build. Perform. Simul. 6 (4) (2013) 269–281.
[73] J. H. Yang, "The Curious Case of Urban Heat Island: A Systems Analsis," Massachusetts Institute of Technology, 2016.
[74] A. Afshari, F. Schuch, P. Marpu, Estimation of the traffic related anthropogenic heat release using BTEX measurements – A case study in Abu Dhabi, Urban Clim 24 (2018) 311–325.
[75] A.K.L. Quah, M. Roth, Diurnal and weekly variation of anthropogenic heat emissions in a tropical city, Singapore, Atmos. Environ. 46 (2012) 92–103.
[76] H. Kusaka, F. Kimura, Thermal effects of urban canyon structure on the nocturnal heat island: Numerical experiment using a mesoscale model coupled with an urban canopy model, J. Appl. Meteorol. 43 (12) (2004) 1899–1910.